Nanoscale Displacement and Strain Measurement

Yong Zhu[1)], Francois Barthelat[1)], Paul E. Labossiere[2)], Nicolaie Moldovan[1)], and Horacio D. Espinosa[1)]
1) Northwestern University, Mechanical Engineering
2145 Sheridan Rd., Evanston, IL 60208-3111
E-mail: espinosa@northwestern.edu
http://clifton.mech.nwu.edu/~espinosa
2) University of Washington, Mechanical Engineering
Box 352600, Seattle, WA 98195-2600

ABSTRACT

The mechanical testing of micro-electro-mechanical systems (MEMS) and nano-electro-mechanical systems (NEMS) requires precise measurements of displacement and strain in the nanometer scale. Integrated testing devices, including specimens, actuators and sensors, were designed and fabricated to overcome the aligning and gripping difficulties faced by previous separated micromechanical testing apparatuses. The specimens were "dog-bone" shaped and were deformed in-plane by electrothermal actuators based on bent-beam suspensions. The displacement field was obtained by comparing surface topologies, acquired with an Atomic Force Microscope (AFM), of undeformed and deformed specimens using the Digital Image Correlation (DIC) method. The change in capacitance of the integrated capacitive sensors was measured to determine the total displacement. The behavior of the whole device was simulated by ANSYS multiphysics, which agreed well with the measured results.

1. INTRODUCTION

Thin films at the micron and sub-micron scales and nanostructured materials (such as carbon nanotubes and nanowires) demonstrate mechanical properties that are different from those of bulk materials. These materials possess the potential to radically impact the industry associated to emerging technologies such as micro/nano-electronics and micro/nano-electromechanical systems (MEMS/NEMS). Their mechanical properties can vary significantly depending on the manufacturing and synthesis conditions, e.g. deposition temperature, etchant concentration, doping and annealing. The reliability of MEMS/NEMS devices is a major issue and can only be assessed by direct measurements on small specimens that are similar in size and must be produced by the same manufacturing processes as the devices. Specimen preparation, force generation and measurement, as well as displacement and strain measurement are the generic challenges in micro and nano-mechanical testing.

Various techniques have been developed to study the mechanical behavior of thin films in the past, including tensile testing [1-4], membrane deflection experiment [5], beam bending [6], nanoindentation [7] and resonance test of microcantilevers [8]. Among these techniques, tensile testing is the most straightforward method and offers more accurate measurements by eliminating the geometry-induced errors. Though, the apparatus for tensile testing is more sophisticated. Two important challenges for tensile testing are: (i) the gripping of specimens, (ii) the measurement of displacement and strain. Electrostatic gripping, adhesive media and micromanipulation have been investigated for the purpose of specimen gripping. Scanning Electron Microscope (SEM) [2-3] and laser interferometer [1] have been employed to measure the displacement, and Digital Image Correlation (DIC) of Atomic Force Microscope (AFM) images [4] has been successfully used to directly obtain strain fields.

All the aforementioned techniques usually require large external testing apparatuses, which rise problems like misalignment and generally limit the specimen size to about tens of microns. MEMS techniques offer the capability of integrating the specimen with the testing system by common micromachining processes, resulting in reduced specimen sizes down to the sub-micron range. MEMS actuation mechanisms include thermal actuation [9], electrostatic actuation [10], and piezoelectric actuation [11]. Capacitive sensing [9], and piezoresistive sensing [12] are commonly used for sensing purpose.

The motivation of this paper comes from the challenges involved by the integration of the tested specimen and testing system in the same MEMS device, and the displacement and strain measurements at nanometer scale. This paper is organized as follows. The integrated testing system, including actuator, sensor and specimen is first described. The preliminary results obtained from DIC analysis of AFM images is then discussed and followed by the ANSYS multiphysics simulation of the whole device. In the end, concluding remarks are given.

2. INTEGRATED TESTING DEVICE

The testing device consists of three parts: a thermal actuator, a specimen and a load sensor based on differential capacitive sensing, as shown in Figure 1. A set of slanted beams connected to a trunk provides the actuation displacement when an electric current is circulated between the two fixed pads. Thermal expansion of the doped polysilicon beams results in a displacement of the trunk and

Proceedings of the 2003 SEM Annual Conference and Exposition on Experimental and Applied Mechanics, June 2-4, Charlotte, North Carolina, Session 77, Paper 155, 2003.

consequently loading of the sample [13]. The load is recorded by the capacitive sensor with nano-Newton resolution. The device is displacement controlled, which is very advantageous in the study of material properties. This type of thermal actuator can be used to generate up to several milli-Newton force. The movement of the movable electrode is equal to the deformation of the folded beams in axial direction. If a voltage bias V_0 is applied on each fixed electrode there will be a voltage change in the moving electrode, V_{sense}, given as:

$$\frac{V_{sense}}{V_0} = \frac{\Delta d}{d} + O(\frac{\Delta d}{d})^3 \quad (1)$$

where d is the gap between movable and fixed electrodes , Δd the displacement of the movable electrodes in the axial direction, and V_0 the bias voltage. In the case that Δd is much smaller than the gap, it is proportional to V_{sense}. If the spring constant of the folded beams is characterized, the force applied on the load cell is then proportional to V_{sense} [14].

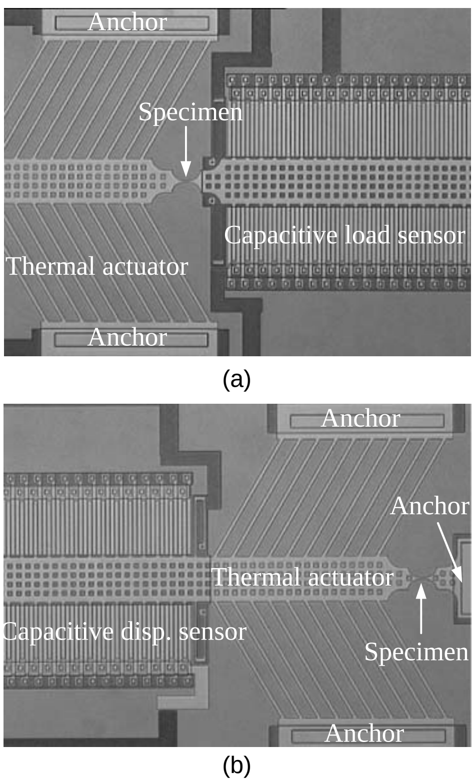

Fig. 1. (a) Optical image of device configuration 1, where the load is measured by the capacitive load sensor and displacement/strain is measured locally. (b) Optical image of device configuration 2, where the capacitive displacement sensor has equal displacement with the specimen.

The specimen can be a carbon nanotube, a nanowire, or thin film. In this paper, polysilicon thin film, a material generally used for MEMS and microelectronics, was tested. For the mechanical testing of thin films, the *in-situ* displacement and strain measurements of the specimens are of significant importance. As a trial version devoted to experiment on displacement/ strain measurements, another configuration was designed, as shown in Figure 2(b). Here, the capacitive sensor has the same displacement as the specimen, given that the thermal actuator moves rigidly. In this configuration, the capacitive sensor was used to measure displacement rather than load. An atomic force microscope (AFM) scanned the specimen surface before and after the loading, and Digital Image Correlation (DIC) processed the AFM data to determine the displacement/strain field. The results can be verified by comparing with electrical measurements performed on the capacitive sensor. In the following sections, experiment and simulation results will be discussed for the device with configuration 2 unless otherwise stated.

The testing devices were fabricated by Multi-User MEMS Processes (MUMPs). The “dog-bone” shape was employed to eliminate stress concentrations. The gauge region of the specimen is 10-μm-long and 4-μm-wide. The thickness of the whole device including the specimen is 2 μm.

3. RESULTS

Surface roughness plays an important role in the mechanical characterization of thin films. Surface roughness is generally associated with the grain size. The grain sizes of polysilicon from different fabrication processes, even different runs of the same process, vary significantly. Figure 2 illustrates two AFM images for the polysilicon films from MUMPs processes at different runs. The left is the device under testing and the right is the device from a previous run. The average roughness values are 10.2 nm and 8.5 nm respectively.

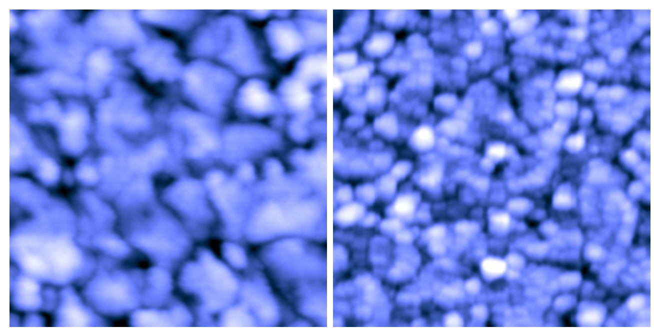

Fig. 2. Two AFM images from two different MUMPs runs indicating the significant variation of grain sizes of polysilicon. The scan areas were 2 μm × 2 μm in both cases.

The displacement and strain fields were determined using AFM scans of the specimen. Figure 3 shows two AFM images of the deformed specimens. The first image was scanned before the induced deformation, when there was no actuation voltage applied. The second image was taken when a 5 V voltage was applied across the thermal actuator. The thermal actuator pulled the specimen in the x direction due to the thermal expansion of the actuator. Because of the symmetry of the entire device, the applied stress in the specimen was uniaxial along the horizontal direction. Moreover, the planarity of the device was investigated with an optical surface profiler and it turned out that the device was flat and parallel to the substrate within 40 nm. This planarity is helpful to remove any out-of-plane force that may be introduced by gripping, which was used in the previous tensile tests. The scanned area was 8 μm × 2 μm within the gauge region. Figure 3(c) shows the displacement field obtained using DIC.

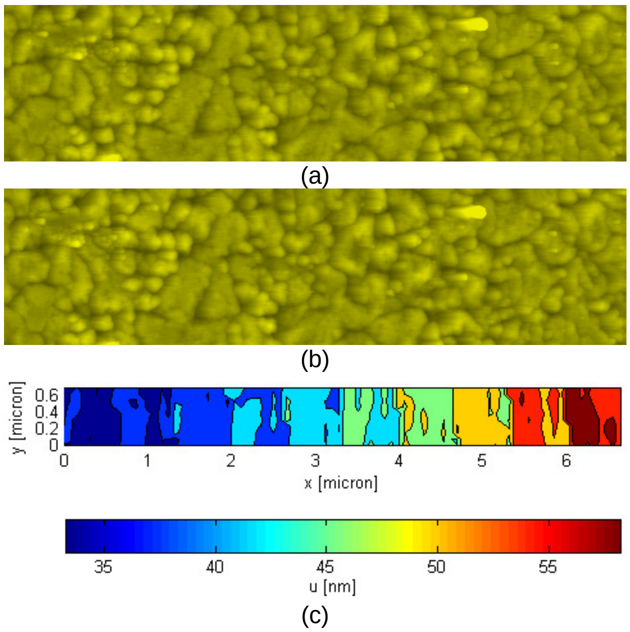

Fig. 3. (a) AFM image of the topography of the specimen surface before loading. (b) AFM image during the loading. (c) Displacement contour computed by DIC within the area shown in (a) and (b). The load was applied in the x direction.

The behavior of the whole device was modeled and simulated using ANSYS/Multiphysics, where structural, thermal and electrical analyses were coupled [15] (Figure 4). The structural boundary condition was to fix all the anchors in X, Y, and Z directions. The thermal boundary condition assumed all the anchors to be at room temperature, since the anchors were connected to the bulk silicon wafer, which served as a constant temperature source. The electrical boundary condition included the 5 volts difference in the top and bottom anchors. It is seen that the displacement of the specimen ranges approximately from 25 nm to 65 nm across the gauge region (Figure 4 (b)). The displacement gradient, i.e. strain is uniform in the gauge region, which is desirable for the mechanical testing of material properties. The simulation result agrees fairly well with the result obtained from DIC analysis of AFM images.

4. DISCUSSION

The data obtained from AFM are not fully repeatable. The drift was a serious problem during the AFM scans. By comparing the two surface topographies obtained from consecutive AFM scans under the same conditions, we observed the “artificial” displacement field, which was caused by the drift. This “artificial” displacement was of the same order of magnitude as the real displacement due to the loading. Through the analyses of extensive consecutive scans, it was observed that the drift was nearly constant. Therefore, it is possible to remove this “artificial” displacement field. The thermal drift was considered the probable cause of this displacement. Noise and other errors due to the hysteresis and non-linearity of the piezoelectric material in the AFM could also be sources of the drift. The further reduction of the drift and other errors is vital and currently under investigation.

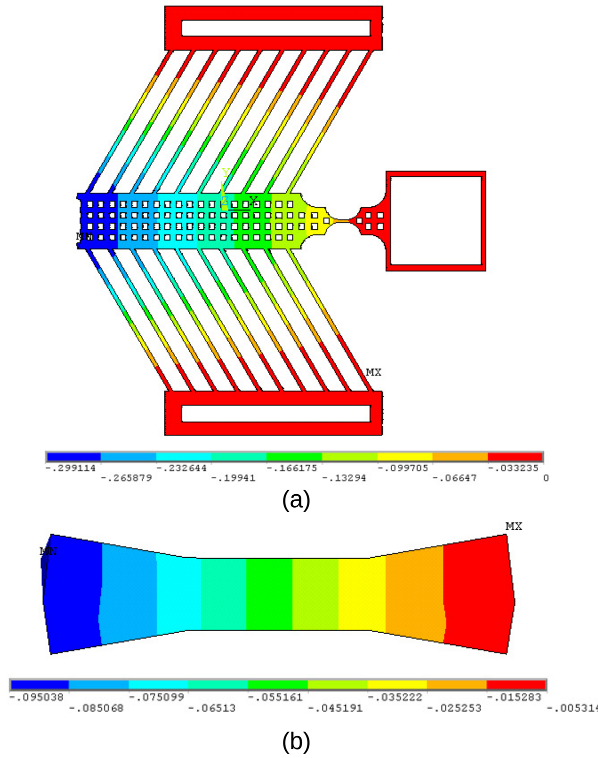

Fig. 4. (a) Displacement contour of the whole device (units in μm), (b) Magnified view of the displacement contour of the specimen at gauge region (units in μm).

5. CONCLUDING REMARKS

An integrated MEMS device has been presented for the mechanical testing of micro and nano scale materials. This device consists of three parts: thermal actuator, specimen, and differential capacitive sensor. Of particular importance are the displacement and strain measurements at the nanoscale. A trial version of the testing device was fabricated and tested for the displacement and strain measurements. Atomic Force Microscopy (AFM) rendered a way to achieve this nanometer resolution with the help of Digital Image Correlation (DIC). The MEMS device was modeled and simulated by ANSYS multiphysics. The preliminary results obtained from AFM/DIC were reported, which agreed fairly well with the results from simulation.

6. ACKNOLEDGMENTS

This work was sponsored by the National Science Foundation (NSF) under Career Award No. CMS-9624364 and Federal Aviation Administration (FAA) under award No. DTFA03-01-C-00031. Special thanks are due to C. Ke for valuable discussions on AFM.

REFERENCES

1. Sharpe, W. N. Jr., Turner, K. T., and Edwards, R. L., “Tensile testing of Polysilicon”, *Experimental Mechanics* **39**, 162-170 (1999).
2. Schweitz, J. Å., and Ericson, F., “Evaluation of Mechanical Materials Properties by Means of Surface Micromachined Structures”, *Sensors and Actuators A* **74**, 126-133, (1999).
3. Tsuchiya, T., Tabata, O., Sakata, J., and Taga, Y., “Specimen Size Effect on Tensile Strength of Surface Micromachined Polycrystalline Silicon Thin Films”, *Journal of Microelectromechanical Systems* **7**, 106-113, (1998).
4. Chasiotis, I., and Knauss, W. G., “A New Microtensile Tester for the Study of MEMS Materials with the Aid of Atomic Force Microscopy”, *Experimental Mechanics* **42**, 51-57, (2002).
5. Espinosa, H. D., Prorok, B. C., and Fischer, M., "A Methodology for Determining Mechanical Properties of Freestanding Thin Films and MEMS Materials", *Journal of the Mechanics and Physics of Solids* **51**, 47-67, (2003).
6. Osterberg, P. M., and Senturia, S. D., “M-Test: A Test Chip for MEMS Material Property Measurement Using Electrostatically Actuated Test Structure”, *Journal of Microelectromechanical Systems* **6**, 107-118, (1997).
7. Nix, W. D., “Thin Film Reviews – Mechanical Properties of Thin Films”, *Metallurgical Transactions A* **20,** 2217-2245 (1989).
8. Kiesewetter, L., Zhang, L. M., Houdeau, D., and Steekenborn, A., “Determination of Young’s moduli of Micromechanical Thin Films Using the Resonance Method”, *Sensors and Actuators A* **35**, 153-159, (1992).
9. Chu, L. L., Gianchandani, Y. B., and Que, L., “Measurements of Material Properties Using Differential Capacitive Strain Sensors”, *Journal of Microelectromechanical Systems* **11**, 489 –498, (2002).
10. Kahn, H., Ballarini, R., Bellante, J. J., and Heuer A. H., “Fatigue Failure in Polysilicon Not Due to Simple Stress Corrosion Cracking”, *Science* **298**, 1215-1218, (2002).
11. Akamine, S., Albrecht, T. R., Zdeblick, M. J., and Quate, C. F., “A Planar Process for Microfabrication of a Scanning Tunneling Microscope”, *Sensors and Actuators A* **23**, 964-970, (1990).
12. Barth, P. W., Pourahmadi, F., Mayer, R., Polydock, J. and Petersen, K., “A Monolithic Silicon Accelerometer with Integral Air Damping and Overrange Protection”, *Tech. Digest of 1988 IEEE Solid-State Sensor and Actuator Workshop*, 35-38, (1988).
13. Fischer, E. E., and Labossiere, P. E., "MEMS Fatigue Testing to Study Nanoscale Material Response," *Proc. of 2002 SEM Annual Conf. & Exp. on Experimental and Applied Mechanics*, (2002)
14. Espinosa, H. D., Zhu, Y., and Peng, B., “A MEMS device for In Situ TEM/AFM/SEM/STM Testing of Carbon Nanotubes and Nanowires”, *Proc. of 2002 SEM Annual Conf. & Exp. on Experimental and Applied Mechanics*, 233-235, (2002)
15. Mankame, N. D., and Ananthasuresh, G. K., “Comprehensive Thermal Modelling and Characterization of an Electro-thermal-compliant Microactuator”, J. Micromech. Microeng. 11, 452-462, (2001).